24th COBEM - 2017

24th ABCM International Congress of Mechanical Engineering
December 3-8, 2017, Curitiba, PR, Brazil

# COBEM-2017-1187
# STUDIES OF HYDRATE ACCUMULATION UNDER MULTIPHASE FLOW CONDITIONS

**Erlend O. Straume**
**Rigoberto E.M. Morales**
Multiphase Flow Research Center – NUEM, Department of Mechanical and Materials Engineering, Federal University of Technology – Paraná, Curitiba, Brazil
erlend.straume@gmail.com, rmorales@utfpr.edu.br

**Xianwei Zhang**
**Giovanny A. Grasso**
**Amadeu K. Sum**
Hydrates Energy Innovation Laboratory, Chemical & Biological Engineering Department, Colorado School of Mines, Golden, CO, USA
xixzhang@mymail.mines.edu, ggrasso0510@hotmail.com, asum@mines.edu

***Abstract.*** *To further obtain insight into the different processes leading to hydrate deposition and blockage formation in different multiphase systems involving gas, oil and water, multiphase flow experiments with hydrate formation were performed in a custom flow loop, focusing on deposition. The experiments were performed for gas + mineral oil + water systems with 50 to 100% liquid loading, liquid and gas velocities that resulted in various flow regimes included stratified flow, stratified-wavy flow, bubble flow and slug flow, and water-cut up to 30%. The hydrate deposition rate at the upper wall depended on direct contact with liquid phases. Experiments that started with no hydrates in the system before cooling resulted in accumulation and bedding of hydrate-covered water droplets shortly after hydrate onset. The bedded hydrates transformed to hydrate deposit during the experiment. The hydrates deposited gradually at both the upper and lower wall of the testing section in the experiments with circulation of hydrate particles before cooling of the testing section. Greater deposition was observed in tests with higher temperature difference between pre-cooling and testing section than with lower temperature difference. Experiments for under-inhibited water with MEG resulted in less deposition than experiments with fresh water at the same water-cut.*

***Keywords:*** *flow assurance, gas hydrates, hydrate deposition, hydrate management*

## 1. INTRODUCTION

“Hydrate Management” strategies in oil and gas production differ from “Hydrate Avoidance” design by ensuring flow and avoiding blockage formation in multiphase flow conditions where hydrates are stable, instead of focusing on preventing altogether hydrate formation. In order to safely implement hydrate management strategies, it is required to study and understand mechanisms and behaviors connected to hydrate formation and accumulation in different multiphase systems involving gas, oil and water. Field tests have demonstrated that hydrate deposition is potentially a major obstacle in safe implementation of hydrate management strategies inside the hydrate formation region (Lachance et al. 2012). This observation resulted in an increased focus on hydrate deposition in the industry and a number of experimental campaigns studying deposition have been performed in later years.

Rao et al. (2013) performed experimental study of hydrate deposition on the outer surface of a cooled pipe exposed to water-saturated natural gas. The study identified growth of hydrates with high porosity until the hydrate layer reached a certain thickness at which the growth stopped and water started filling the porous space decreasing porosity and hardening the deposit. Recent experimental studies of hydrate deposition in annular gas-water flow in a pipe testing section at various subcooling conditions indicated some disagreement with simple model of increased pressure drop due to hydrate film growth (Di Lorenzo et al., 2014). The authors suggest that additional hydrate phenomena not considered in the model like particle deposition from the liquid or deposit sloughing from the wall made significant contributions to the pressure drop.

Grasso et al. (2014) performed laboratory experiments in a rocking cell studying hydrate deposition in mineral oil and gas condensate systems as well as 100% water cut system. These experiments indicated that water could reach the deposition surface by direct contact between the water phase and the cold surface, by condensation of water on the surface, and by liquid capillarity. Straume et al. (2016) studied hydrate formation and deposition mechanisms for systems with non-emulsifying oil and condensate in the same rocking cell apparatus. These experiments showed that before hydrate formation the oil and water phases formed a shear stabilized dispersion, which separated upon hydrate formation onset.

This paper describes observations and measurements from an experimental campaign performed in a custom flow loop focusing on deposition with objective to further obtain insight into the different processes leading to hydrate deposition and blockage formation in multiphase systems involving gas, oil and water.

## 2. EXPERIMENTAL METHODE

The experiments were performed in a high-pressure miniloop installed in the laboratories of Colorado School of Mines. The miniloop (Figure 1) was constructed as part of the Ph.D. study of Grasso (2015) and funded by DeepStar. It has a maximum operating pressure of 50 bar and the temperature of fluids can be controlled between 0 and 25 °C during flowing conditions. The main components of the miniloop are: (1) Gas and water injection pumps (2) vertical separator, (3) gas and liquid circulation pumps, (4) gas and liquid flow meters, (5) precooling pipes with thermal insulation (cooling jacket), (6) 31 inches long and two inch inner diameter testing section with cooling the upper and lower wall, and inspection windows in the sides for video recording and observation of flow patterns and formation of hydrates, (7) pressure and temperature measurements (8) thermostatic baths for cooling the testing section and precooling pipes, and (9) National Instruments data acquisition system connected to a LabVIEW® (National Instruments, 2012) based logging software (not included in the figure). The flow directions are indicated with arrows in Figure 1. The blue arrows indicate the flow of liquid, the red gas flow and green show two-phase flow of gas and liquid.

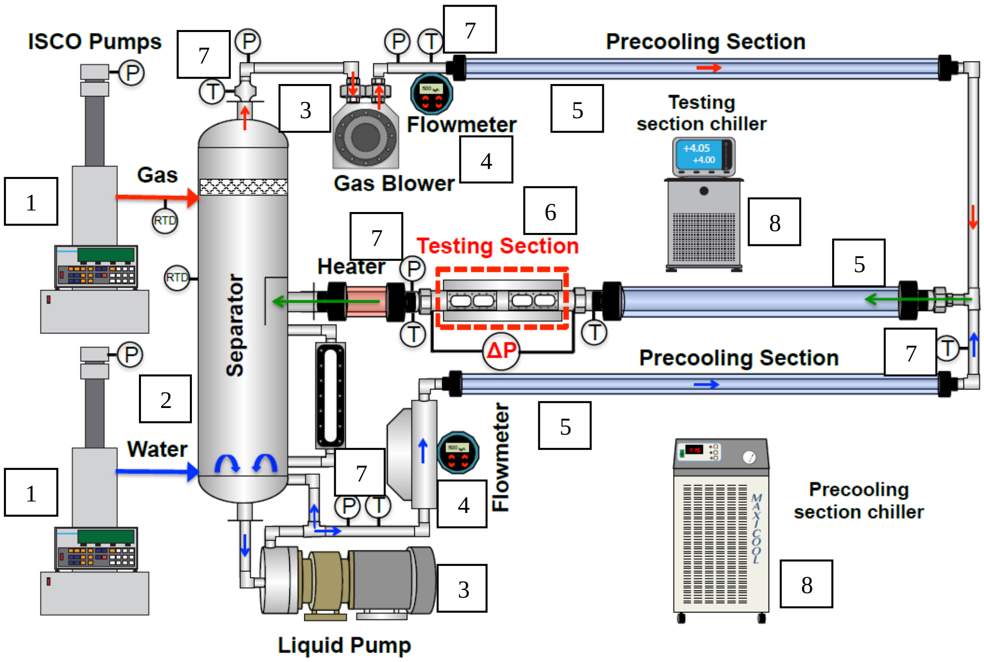


Figure 1. The miniloop installed in the laboratory of the Colorado School of Mines. (Grasso, 2015)

### 2.1 Experimental Procedure

The miniloop was charged with the required volume of mineral oil 70T at atmospheric conditions and pressurized with the gas mixture (74.7% methane and 25.3% ethane) in the beginning of the experimental campaign. Gas pressure and added gas volume could be controlled by an ISCO pump during the experiments. Water was added to with an ISCO pump at pressurized conditions increasing the water cut from 0 to 30% during the experimental campaign. 6.6 wt.% MEG was added to the water phase for the two last experiments. In order to study how different shear and mixing of phases influenced deposition rate, the liquid and gas velocities were adjusted in the start and during the experiments to achieve the desired flow patterns, which in these experiments included stratified flow, stratified-wavy flow, bubble flow and slug flow.

Two different dissociation procedures were implemented before the experiments, which appear to have influenced the way hydrates formed in the testing section in the beginning of subsequent tests. The normal procedure involved heating the entire flow loop to temperatures higher than hydrate equilibrium in order to dissociate all hydrates in the system. The experiment was started by changing the set point temperature of the testing section and the pre-cooling section to temperatures lower than hydrate equilibrium. The temperature set point of the testing section was set to a temperature lower than the pre-cooling section (2 °C temperature set-point difference in the majority of the experiments). An alternative dissociation procedure was implemented prior to some of the experiments: hydrates in the testing section were completely dissociated while the temperature of the pre-cooling sections remained lower than hydrate equilibrium temperature to preserve some of the hydrates in the system. The experiments were initiated by changing the temperature settings to the same as in the experiments that did not have hydrates in the system before hydrate formation in the testing section.

### 2.2 Experimental Conditions

The miniloop experiments were performed with a gas mixture composed of 74.3% methane and 25.7% ethane, mineral oil 70T and fresh water or water with 6.6 wt.% MEG at about 4 MPa pressure. Other experimental conditions for are given in Table 1.

Table 1. Experimental matrix for hydrate deposition experiments in the miniloop.

| Exp. No. | Water cut [%] | Testing section temp. [°C] | Pre-cooling temp. [°C] | Flow pattern | Additional conditions |
|---|---|---|---|---|---|
| 1 | 0 – 10 | 0 – 10 | 0 – 10 | 100% liquid | Circulation of hydrates during water injection |
| 2 | 10 | 8 | 2 | Stratified | Circulation of hydrates, problems with pre-cooling |
| 3 | 10 | 6 | 0 – 10 | Stratified | Circulation of hydrates, problems with pre-cooling |
| 4 | 10 | 4 – 10 | 5 – 8 | Stratified | Circulation of hydrates |
| 5 | 10 | 4 | 6 | Stratified | Circulation of hydrates, shut-in and re-start |
| 6 | 10 | 4 | 6 | Stratified | No hydrates before cooling of testing section and pre-cooling |
| 7 | 10 | 4 – 9 | 6 | Stratified | Formation of hydrates at 6 °C pre-cooling and 9 °C testing section and 4 °C cooling testing section after hydrate onset |
| 8 | 10 | 4 | 6 | Bubble flow | No hydrates before cooling of testing section and pre-cooling |
| 9 | 10 | 4 | 6 | Stratified / bubble flow | Circulation of hydrates before cooling of testing section to 4 °C |
| 10 | 20 | 4 | 6 | Stratified / bubble flow | Circulation of hydrates before cooling of testing section to 4 °C |
| 11 | 30 | 4 | 6 | Bubble flow | Circulation of hydrates before cooling of testing section to 4 °C |
| 12 | 30 | 2 | 6 | Slug flow / bubble flow | No hydrates before cooling of testing section and pre-cooling |
| 13 | 30 | 2 | 6 | Slug flow / bubble flow | Shut-in and re-start |
| 14 | 30 | 1 | 5 | Slug flow / bubble flow | 6.6 wt.% MEG in water |
| 15 | 30 | 1 | 5 | Slug flow / bubble flow | 6.6 wt.% MEG in water |

## 3. RESULTS AND DISCUSSION

### 3.1 Flow regime

Figure 2 shows images of hydrate deposits in the testing section after finishing (a) Experiment 4 with stratified flow and about 50% liquid loading (LL) and (b) Experiment 9 with bubble flow and 50-100% LL. As shown in these images, hydrate deposits were almost absent from the upper wall in experiments with a stratified flow regime in which the liquid was not in direct contact with the upper wall, while there was considerable amount of deposits also at the upper wall in tests with bubble and slug flow. These observations indicates that direct contact between liquid phases in the flow loop and a pipe surface area in the testing section promoted deposition of hydrates on this surface area.

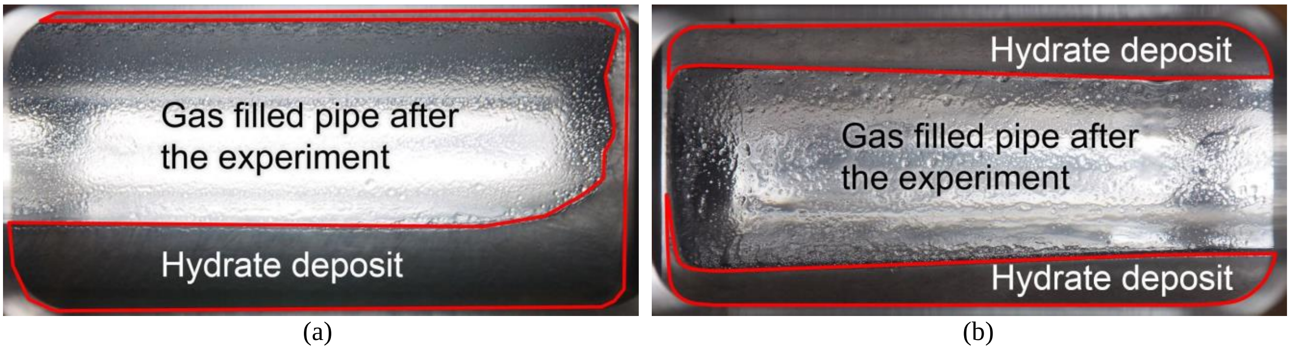


Figure 2. Images of hydrate deposits (outlined in red) in the testing section after finishing (a) Experiment 4 and (b) Experiment 9. The window area in the images is 68 x 34 mm.

### 3.2 Experiments without hydrates before cooling of the testing section

The water phase was fully dispersed in the oil due to shear from the flow before hydrate formation onset in the experiments that followed the procedure of dissociating all hydrates in the system before cooling of the testing section to temperatures lower than hydrate equilibrium. Shortly after hydrate onset, agglomerates of hydrate-covered water droplets started flowing along the bottom of the pipe. These hydrates bedded and accumulated in the testing section, blocking flow in 60% or more of the pipe cross section (Figure 3 a). After reaching a maximum visual hydrate volume between 20 minutes and 1 hour after hydrate onset, the volume of the hydrates in the lower part of the testing section decreased slowly to less than half of the maximum volume as the accumulated hydrate-covered water droplets transformed to solid hydrate deposits. Pressure drop over the testing section also reached maximum during this first hour of the experiment as demonstrated in Figure 4. (The pressure increased between 5 and 21 hours after start of the experiment due to blockage of the gas flow during this period.) The temperature difference between the inlet and outlet of the testing section was 2 – 3 °C throughout the experiment. Hydrates deposited slowly at the upper pipe surface during the experiments, and the visual deposit volumes at the upper and lower pipe surfaces were similar in the end of the experiments as shown in Figure 3 b. The hydrate formation and accumulation mechanisms in this experiment could be considered a combination of agglomeration, bedding and deposition. The observation of the hydrate covered water droplets separating from the oil-water dispersion might be related to detection of phase separation due to hydrate formation in rocking cell experiments performed with mineral oil 70T as oil phase (Straume et al., 2016).

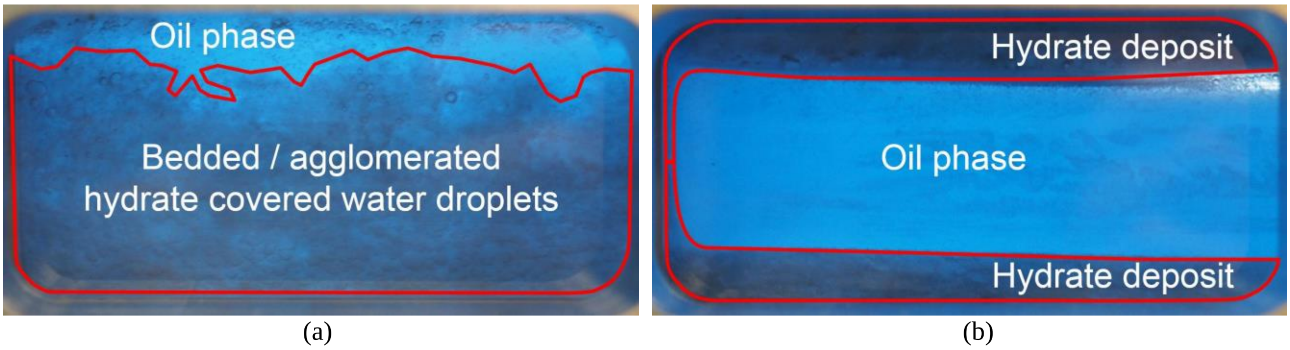


Figure 3. Images of (a) accumulated hydrates in the testing section about 20 minutes after hydrate onset and (b) hydrate deposits in the testing section 49.5 hours after hydrate onset. Both images were taken during Experiment 8. The window area in the images is 68 x 34 mm.

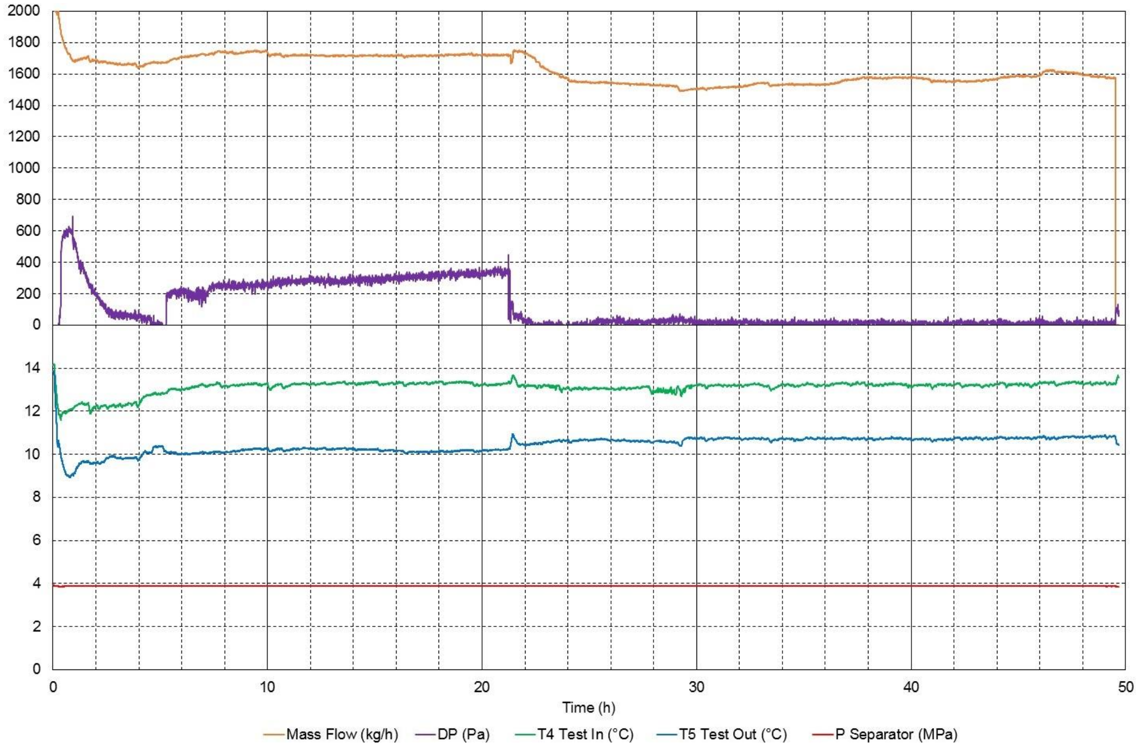


Figure 4. Measured parameters from Experiment 8.

### 3.3 Experiments with recirculation of hydrates before cooling of the testing section

In the experiments with recirculation of hydrate particles before cooling of testing section, a separate water phase was observed flowing in the bottom of the pipe in the beginning of the experiments, but water was also dispersed in the oil phase. As shown in Figure 5, hydrates deposited gradually at both the upper and lower wall from the time the cooling temperature of the testing section was set to a temperature lower than the pre-cooling section in experiments with a flow regime permitting direct contact between the liquid phases and the entire pipe wall. The hydrate formation and accumulation mechanism in these experiments was most likely a combination of hydrate film growth at the pipe wall and deposition of hydrate particles from the flow on the water wetted pipe wall. By comparing experiments 8 and 9 shown in figures 3b and 5b respectively, it can be concluded that the volumes of the hydrate deposits in the two experiments were similar. This shows that circulation of hydrates had little influence on the end volume of hydrate deposit when flow pattern, water cut and cooling conditions for the testing section and precooling section were the same throughout the two experiments. However, the difference between the rapid accumulation of hydrates in the beginning of the experiment without hydrates before cooling of testing section and the gradual deposition throughout the experiment with circulation of hydrates is an observation that might be of importance in development of hydrate management methods.

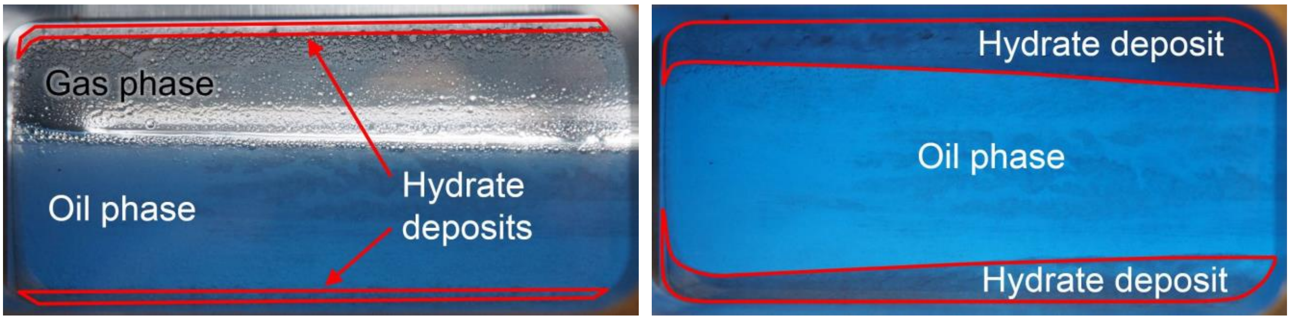


(a) (b)

Figure 5. Images of (a) hydrate deposits about 1 hour after starting cooling of testing section and (b) hydrate deposits in the testing section 46 hours after starting cooling. Both images were taken during Experiment 9. The liquid loading in the pipe varied between 50 and 100% during this experiment due to instable gas flow rate. The window area in the images is 68 x 34 mm.

### 3.4 The influence of water cut on hydrate deposition

Figure 6 show the deposits in the last window frame of the testing section in the end of experiments 9, 10 and 11 with water cuts of 10, 20 and 30% respectively. The testing section was cooled to 4 °C, the pre-cooling section was cooled to 6 °C, the flow pattern ensured liquid wetting of both upper and lower surface in the testing section, and hydrates were circulated before cooling of testing section. Although the volume of the deposit seems to be slightly higher for Experiment 9 compared to experiments 10 and 11, the water cut does not seem to have much impact on the thickness of the deposits in the end of these experiments. A possible limitation of the hydrate deposit thickness in these experiments could be the heat transfer through the deposit. One probable hypothesis is that the deposition of hydrates at the wall continued until the temperature at the deposit surface reached hydrate equilibrium. Given that the flow and temperature conditions were similar for these three experiments the temperature at the deposit surface would reach equilibrium at similar deposition thickness as shown in Figure 6.

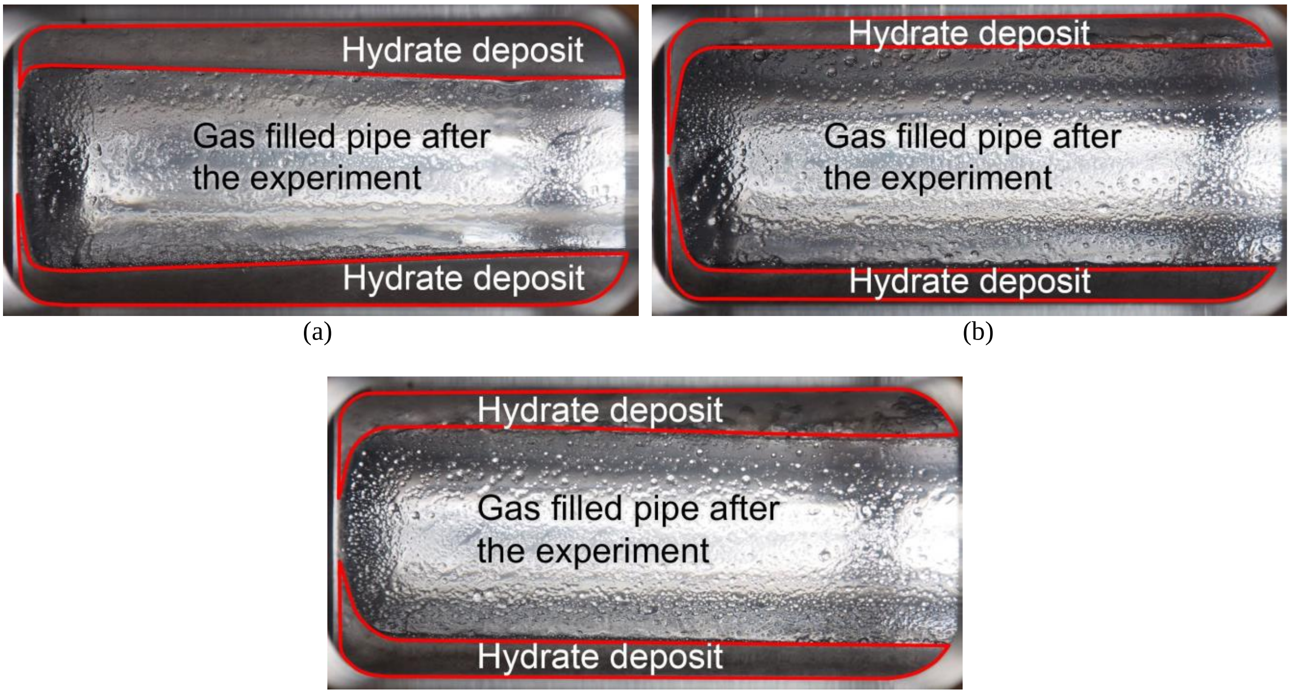


(a) (b) (c)

Figure 6. Images of hydrate in last window of the testing section after the liquid phases were drained from the pipe in the end of (a) Experiment 9, (b) Experiment 10, and (c) Experiment 11.
The window area in the images is 68 x 34 mm.

### 3.5 The influence of temperature difference on hydrate deposition

Experiments 12 and 13 were performed with 30% water cut, cooling of the testing section to 2 °C, cooling of the pre-cooling to 6 °C, and no hydrates before cooling of testing section. In a similar manner as Experiment 8, agglomerates of hydrate-covered water droplets started flowing along the bottom of the pipe shortly after hydrate onset. These hydrates bedded in the testing section and were transformed to continuous a hydrate deposit. There was an increase in pressure drop during the first hour similar to Experiment 8. Hydrates deposited at the upper pipe surface and the window surfaces in addition to the lower part of the pipe reducing the cross section area available for flow, which caused the pressure drop over the testing section to increase to about 1000 Pa at a flow rate between 600 and 800 kg/h. The temperature difference between the inlet and outlet of the testing section increased to about 5 °C, which might be explained by the lower flow rate. There were considerable more deposit in the end of these experiments than in the previous experiments with lower temperature difference as seen in Figure 7. There were no significant difference between the two experiments that were run under these cooling conditions. This might be due to dissociation of all hydrates during shut-in and rapid mixing of oil and water phases during restart, which resulted in similar conditions in the beginning of the two experiments.

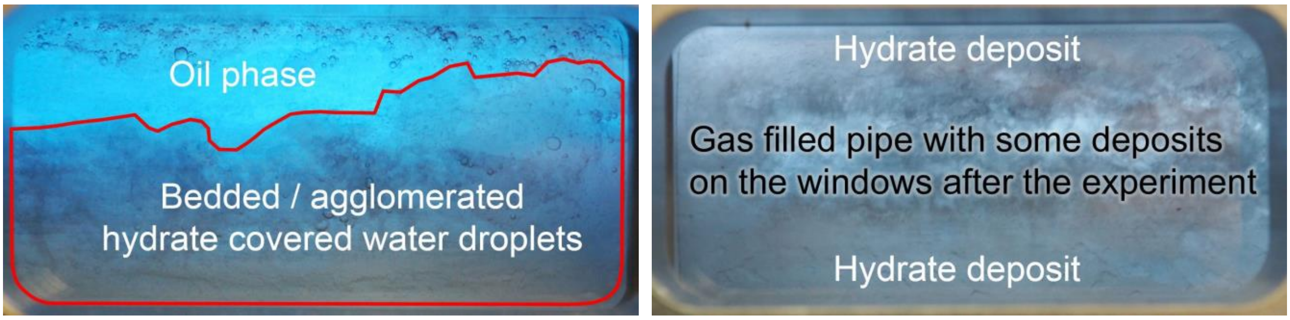


(a) (b)

Figure 7. Images of (a) bedded hydrate about 1 hour after starting cooling of testing section and (b) hydrate deposits in the testing section in the end of the experiment after draining liquids from the pipe. The images were taken during in the end of Experiment 12. The window area in the images is 68 x 34 mm.

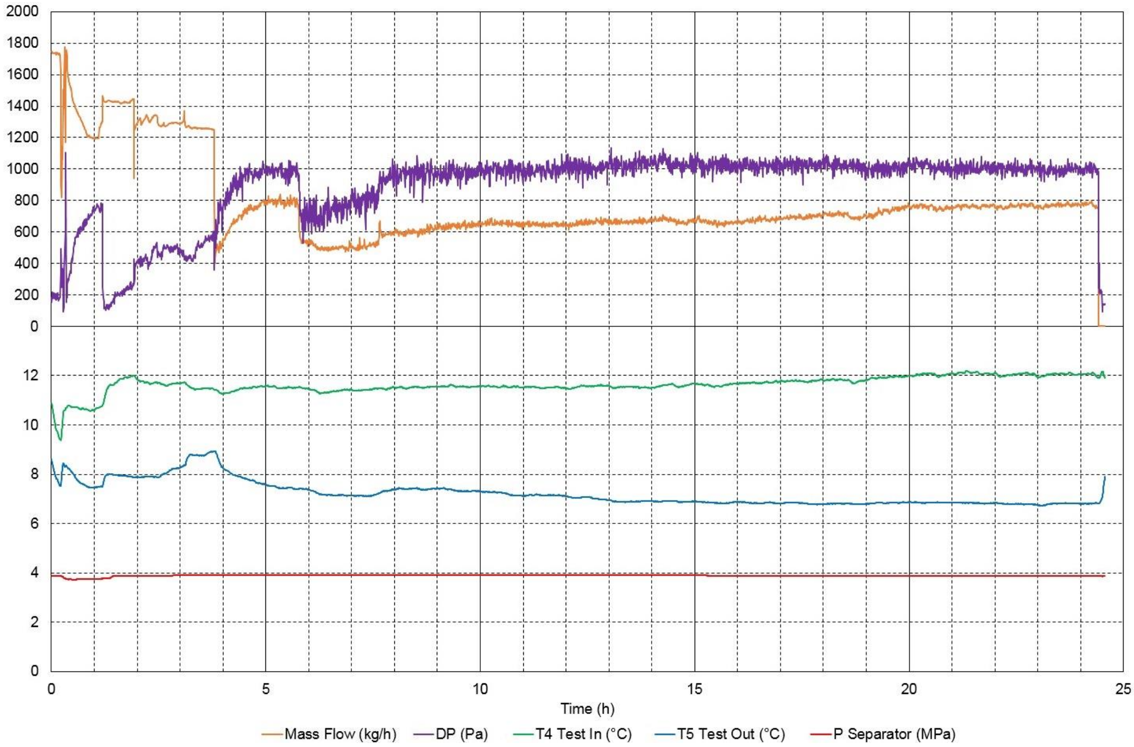


Figure 8. Measured parameters from Experiment 12.

### 3.6 The influence of under-inhibited system with MEG

Hydrate started depositing at the upper and lower surfaces of the testing section shortly after start of the experiments with 30% water cut with 6.6 wt.% MEG in the water, cooling of the testing section to 1 °C, cooling of the pre-cooling to 5 °C, and no hydrates before cooling of testing section. The oil phase contained dispersed hydrates and water that likely caused increased viscosity shortly after hydrate formation onset. Slug flow with altering gas and liquid phase could be seen flowing behind the deposits at the window in the upper part of the testing section as shown in Figure 9a. These experiments for under-inhibited water with MEG resulted in less deposition than experiments with fresh water at the same water-cut and 4 °C temperature difference between the pre-cooling and testing section as seen in Figure 9b. During the majority of Experiment 14, the pressure drop over the testing section was about 400 Pa (less than half of Experiment 12) and the flow rate was about 1500 kg/h (about twice as high as Experiment 12), which also indicates considerably lower deposit volume. Porous regions were observed inside the formed hydrate deposit in the under-inhibited experiments, possibly filled with unconverted water-MEG solution with a higher MEG concentration due to water consumed in hydrate formation in the proximity to these porous regions.


(a) (b)

Figure 9. Images of (a) hydrate deposits and bedded hydrate about 1 hour after starting cooling of testing section and (b) hydrate deposits in the testing section in the end of the experiment after draining liquids from the pipe. Both images are from Experiment 14. The window area in the images is 68 x 34 mm.

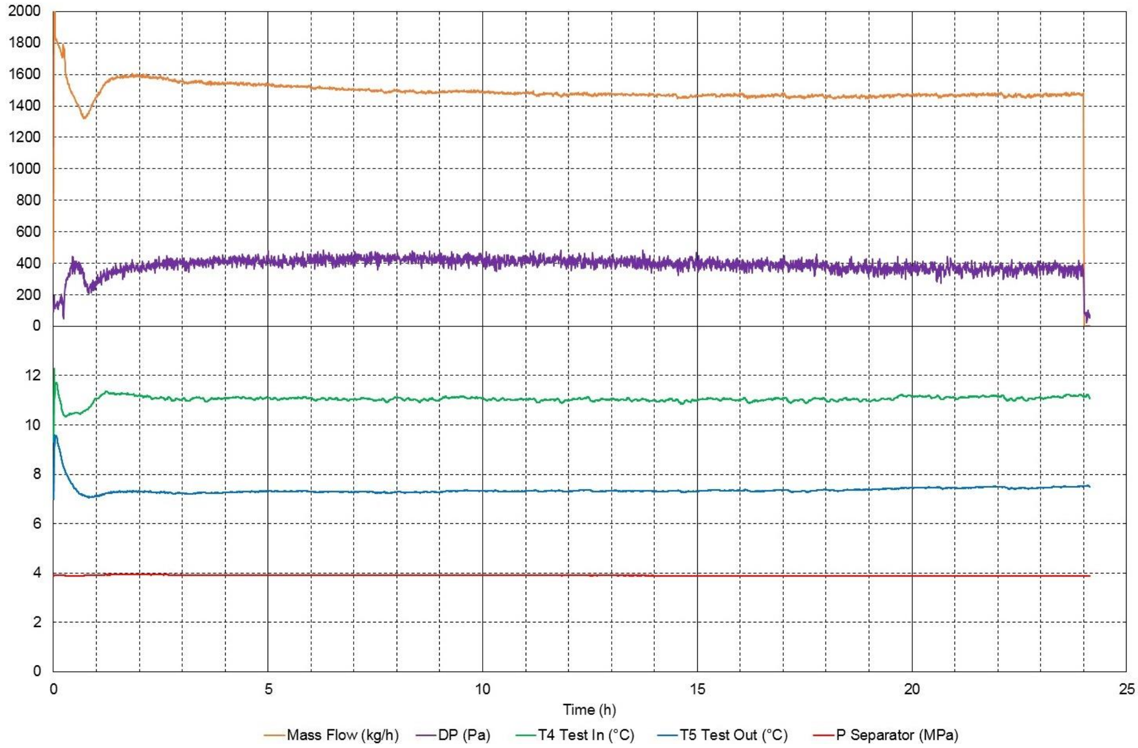


Figure 10. Measured parameters from Experiment 14.

## 4. CONCLUSIONS

Hydrate deposition rate at the upper wall depended on direct contact with liquid phases. There were small differences between hydrate deposit volumes in experiments with water cuts of 10, 20 and 30% with set point of testing section at 4 °C and pre-cooling at 6 °C. Significantly more hydrate deposition was observed in experiments higher subcooling and temperature gradient in the system with set point of testing section at 2 °C and pre-cooling at 6 °C. Rapid accumulation and bedding of hydrate-covered water droplets shortly after hydrate onset was observed in experiments with no hydrates in the system before cooling. Experiments with the same cooling conditions and circulation of hydrates before cooling to experimental temperatures resulted in slow and gradual deposition at the upper and lower surface of the testing section. This difference in deposition behavior might be important for hydrate management strategies. Experiments with under-inhibited system with MEG resulted in lower deposition at similar subcooling and temperature gradient in the system compared to un-inhibited system with fresh water.

## 5. ACKNOWLEDGEMENTS

This work was funded by Repsol Sinopec Brasil supported by ANP – The National Agency of Petroleum, Natural Gas and Biofuels, Brazil. Giovanny A. Grasso, currently working for ExxonMobil Production Company, Houston, TX, USA, constructed the high-pressure miniloop as part of his Ph.D. study. The construction of the miniloop funded by DeepStar.

## 6. REFERENCES

Grasso, G. A., Sloan, E. D., Koh, C. K., Sum, A., & Creek, J. L., 2014. "Hydrate Deposition Mechanisms on Pipe Walls". In *Proceedings of Offshore Technology Conference – OTC 2014*. Houston, TX, USA.

Grasso, G.A., 2015. *Studies on the growth of the frost layer based on heat and mass transfer through porous media*. Ph.D. thesis, Collorado School of Mines, Golden, CO, USA.

Lachance, J.W., Talley, L., Shatto, D.P., Turner, D.J., and Eaton, M.W., 2012, "Formation of Hydrate Slurries in a Once-Through Operation". *Energy & Fuels*, Vol. 26, No.7, p. 4059-4066.

Rao, I., Koh, C.A., Sloan, E.D., & Sum, A.K. 2013, "Gas Hydrate Deposition on a Cold Surface in Water-Saturated Gas Systems ". *Industrial & Engineering Chemistry Research*, Vol. 52, No. 18, p. 6262-6269.

Straume, E.O., Kakitani, C., Merino-Garcia, D., Morales, R.E.M., and Sum, A.K., 2016, "Experimental Study of the Formation and Deposition of Gas Hydrates in Non-Emulsifying Oil and Condensate Systems". *Chemical Engineering Science*, Vol. 155, p. 111-126.

## 7. RESPONSIBILITY NOTICE

The authors are the only responsible for the printed material included in this paper.